Journal of the Korean Nuclear Society
Volume 29, Number 4, pp. 269~279, August 1997

On the Sampling and Transport of Radioactive Aerosols from Waste Thermal Process

Hee-Chul Yang and Joon-Hyung Kim
Korea Atomic Energy Research Institute
150 Dukjin-dong, Yusong-gu, Taejon 305-353, Korea

Yong Kang
Chungnam National University
220 Gung-dong, Yosong-gu, Taejon 305-764, Korea

(Received September 16, 1996)

Abstract

The errors associated with incorrect sampling and transport of radioactive aerosol from radwaste thermal process off-gas are analyzed and the conditions of representative sampling and correct transport of radioactive aerosol for off-gas system evaluation are discussed. An estimation method of sampling errors for individual radionuclides is proposed and applied to simulated vitrification melter aerosols. Prediction methods for particle deposition in sample transport tube under laminar as well as turbulent flow conditions are also described by example calculations with simulated incinerator off-gas. From the results of example calculations and plots, instrumental and operational conditions of radioactive aerosol sampling system with minimized errors and correction methods for nonideal sampling and transport are recommended.

1. Introduction

Characterization of radioactive aerosol in the process stream of radwaste thermal treatment plants such as incineration and vitrification plant, which are under developing or commercialization in Korea [1, 2], is necessary to evaluate the process safety factors such as nuclide volatilities in the furnace or melter, removal efficiencies through off-gas system units and emission concentrations in stack. Unfortunately, direct measurement of radioactivity of aerosol particle in the process stream is impossible even with currently well-developed radioactivity measuring instruments. Therefore the problems of representative sampling and correct transport of radioactive aerosols to the instrument often occur.

Standard methods and guidelines for aerosol sampling have not given full information on aerosol behavior associated with errors during sampling and transport of aerosol. The recommended conditions are only ideal but practically not accessible for radioactive aerosol measuring system, especially in radwaste thermal process. However, there have been many experimental and theoretical investigations, which can be applied for correction or estimation of errors due to unideal sampling and transport conditions.

Badzioch [3] discussed methods of interpreting sampling data taken under anisokinetic conditions.

Hemeon and Haines [4] found experimentally that errors in the calculated particle concentration can range from 40 to 60% when the suction velocity ranges from two-thirds isokinetic to twice isokinetic. Davis [5], Rehm [6] and Herman [7] also experimentally investigated this effect. All of them described the influence of particle inertia on the efficiency as a function of Stokes number. The results are very similar. Vitols [8] and Ruping [9] attributed sampling errors to three different sources-inertial effect, deposition in the sampling channel and particle bounce from the front edge of the probe. They determined the sampling efficiency due to the first of these effects only using a photographic techniques.

A number of theoretical and experimental investigations on aerosol particle deposition have been performed in numerous engineering applications arising from the needs of the microelectronic and computer industries and protective coat industries. Mass diffusion in laminar flows is a relatively well established [10]. Extensive reviews of earlier and recent development of theories of turbulent deposition process and experimental studies were provided by Wood [11] and Papavergoes and Hedley [12].

Previous research works related to aerosol sampling efficiency have been concerning on the mass concentration of particles. There has been no interpretation on sampling errors on the measurement of individual element or nuclides. In radwaste thermal system, it is necessary to know the concentration of each nuclide in the aerosol since the behavior of individual radionuclides have to be known to evaluate system status such as volatility, particle entrainment, removal efficiency, final emission of the individual nuclides. The correction methods for the measured concentration of individual nuclides for anisokinetic sampling conditions are proposed in this paper. In addition, some graphical illustrations of deposition in the sample transport tubes under various sample transport conditions were also described with generally accepted deposition models and the results were analyzed in order to present sample transport conditions with minimized error.

2. Radioactive Aerosol Measuring System

It is possible to analyze radioparticles in off-gas only after aerosol sample has been transported to radioactivity detection instruments and there is a spacial distance between the site of sampling and the instrument in which the radioactivity analysis is performed. This concept of radioactive aerosol particle measurement system is shown in Fig. 1. For measurement of radioactivity of aerosol particle in duct flow, we normally take only a part of the aerosol sample and expect it to be a representative sample. If the radioactivity of aerosol is homogeneous in total flow, this can be true. Radioactive aerosols in a room or flowing through a duct is normally inhomogeneous. The approach to increase homogeneity is to increase the number of sampling points distributed in the total aerosol as well as the volume of aerosol sample. Some guidelines or standard methods such as Korean Test-Methods for Pollution Process, German VDI-Guideline 2066, USEPA's air sampling methods and Japanese JIS-8808 have agreed upon minimum required numbers of sampling points of aerosol flow in a duct or stack. For sampling from still gas, we can refer to an article by Agarwal and Liu [3].

Depending on the properties of the investigated radioactive aerosol and measuring range of the instrument, it may also be necessary to condition aerosol particle so that the properties and geometry of sampled radioparticles match the requirements of the radioactivity detection instrument. In general, ultimate conditioning of radioactive aerosol particle is an accumulation of radioparticles on a flat HEPA sampling filter, increasing radioactivity with known aerosol sample volume. The main requirement causing sample transport error is the necessity of installation of commercial instrument in clean room, which is distant from sampling site. Therefore it is impossible to achieve completely representative sample even with self-regulating isokinetic sampler since loss of aerosol

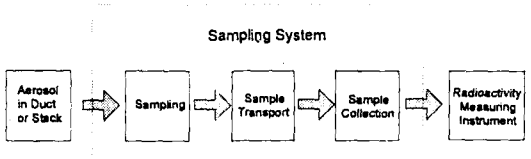

Fig 1. Schematic Diagram of Radioactive Aerosol Sampling and Measuring System

particle occurs in relatively long sample transport line in radioactive aerosol measuring system. In addition, conventional self-regulating isokinetic sampler can not be adequately installed for hot process off-gas from waste thermal process [13, 14]. Therefore we have to know the difference between the aerosol concentration in process flow and that in sample flow as well as the deposition in sample transport line. In order to know whether the resulting errors are acceptable with respect to the requirements, the effects of sources of error during sampling and transport of aerosol have to be quantitatively estimated [15, 16].

3. Sampling Efficiency of Radwaste Thermal Process Aerosols

3.1. Characteristics of Radwaste Thermal Process Aerosols

The sampling efficiency can be quantified by determining the ratio of the concentration in the sample to the concentration in the investigated aerosol. This ratio is referred to as sampling efficiency or suction efficiency η. If the radioactivity of the particle is in proportion to the particle mass, sampling efficiency for radioactive aerosol can be described as,

$$\eta = \frac{C_{m,s}}{C_{m,g}} = \frac{C_{a,s}}{C_{a,g}} \quad (1)$$

where $C_m(kg/m^3)$ and $C_a(Bq/m^3)$ are mass and radioactivity of the sampled particles in unit sample gas volume, respectively, and subscript 's' and 'g' represent sample and process off-gas, respectively. For a representative sample, η is equal to unity. The sampling efficiency largely depends on the properties of particles, especially on particle size. A detailed efficiency has to be investigated with fractional sampling efficiencies as a function of particle diameter, d_p ($\eta = f(d_p)$). Therefore Eq. (1) is only true if the normalized size distributions are equal to radioactivity distributions. In radwaste thermal treatment system such as incineration or vitrification system, radioactivity distributions of aerosol particles in off-gas are much different from particle size distributions. This is mainly caused by two different formation routes of radioactive aerosol particle. Semivolatile nuclides such as Cs, Ru and Te, are readily volatilized in the furnace or melter and are mostly entrained as gaseous nuclides into the off-gas. Entrained gaseous semivolatile nuclides condense into particulate during off-gas cooling period. Regardless of whether the volatilized nuclides condense by heterogeneous or homogeneous route, they ultimately end up as submicron particles [17, 18]. Other route of radioactive aerosol source in waste thermal process is particle entrainment in the off-gas. Nonvolatile nuclides such as Co and Mn are entrained by combining with fly ash particles. Although the smaller fly ash particle tends to become entrained in the off-gas, the entrained fly ash particles are still relatively much larger than fine condensed semivolatile particle.

3.2. Errors Due to Anisokinetic Sampling

Gas flow patterns for isokinetic and anisokinetic sampling conditions are shown in Fig. 2. Large errors may resulted from anisokinetic operation of sampling probes during aerosol sampling. The main reason for this is that the large particles in high flow rate, because of their inertia, do not follow the changed gas flow line due to anisokinetic sampling but tend to continue on their original path. Therefore the more difference between off-gas velocity v_o and suction velocity v_s results in the greater sampling error.

The influence of particle inertia on the efficiency is

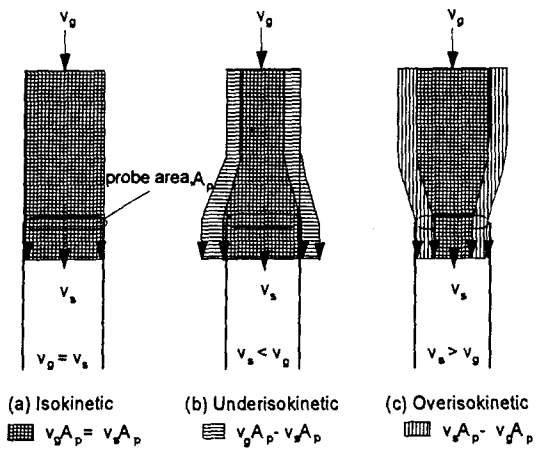

Fig 2. Gas Flow Patterns for Isokinetic and Anisokinetic Sampling Conditi

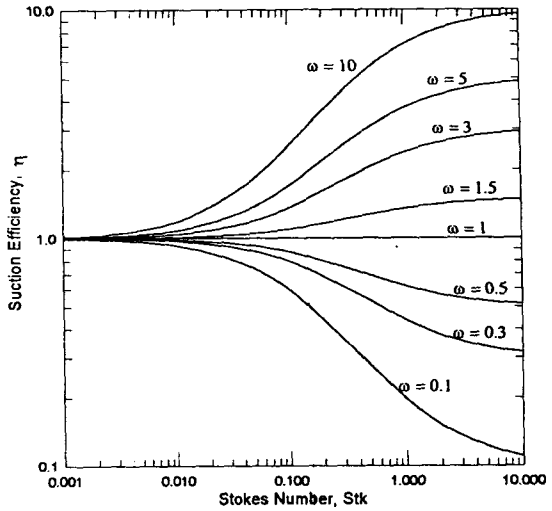

Fig 3. Aerosol Sampling Efficiencies with a Stokes number for Given Suction Velocity Ratio

described as a function of velocity ratio between suction velocity $v_s(ms^{-1})$ and off-gas velocity $v_g(ms^{-1})$, ω $(=v_g/v_s)$ and Stokes number, $Stk(-)$; $\eta = f(\omega, Stk)$. For large particle that has sufficient inertia, the Cunningham correction factor can be regarded as unity and thus the Stokes number is calculated from :

$$Stk = \frac{\rho_p \, d_p^2 \, v_s}{(18\mu \, D_p)} \tag{2}$$

where $\rho_p(kgm^{-3})$ is particle density, $d_p(m)$ particle diameter, $\mu(kgm^{-1}s^{-1})$ viscosity of the gas and $D_p(m)$ the probe diameter. For example calculation, we employed here the method by Belyaev and Levin [8, 9] :

$$\eta = 1 + \frac{(\omega - 1)(2\omega + 0.62)}{(\omega \, Stk^{-1} + 2\omega + 0.62)} \tag{3}$$

The calculated sampling efficiency η as function of the Stokes number Stk for different velocity ratio ω is shown in Fig. 3. In this figure, several discussions can be drawn ; We should try to make the velocity ratio ω close to unity, by adjusting the suction velocity v_s. A ratio smaller than unity causes smaller errors than a ratio larger than unity. For a constant flow rate, an increase of probe diameter D_p reduces the Stokes number. Therefore, when we measured particle size distributions with a constant flow rate through cascade impactor, the diameter of the probe should be enlarged. The errors become small since the impactor probe sample from reduced flow gives a smaller Stokes number. The sampling errors are also affected by the gaseous composition of the aerosol as well as temperature, since the Stokes number is a function of gas density and viscosity. Since the sampling errors become less for smaller Stokes numbers, the higher temperature will reduce sampling errors.

Several kinds of self-regulating isokinetic sampler have been developed in order to cope with ever-changing off-gas velocity. However, most of them can not be properly installed to sample hot process off-gas with high particle concentration since they have originally developed for measurement of dust emission in stack. Therefore we should continuously check the fluctuation of off-gas velocity at sampling position for future correction. We should continuously record off-gas linear velocity as well as sampling flow rate, since sampling flow rate becomes lower than set sampling flow rate due to increased pressure drop across sampling filter with sampling time. If we know particle size distributions of investigating aerosol, we can correct sampling error due to anisokinetic sampling with velocity ratio. Even if there

have been no developed available data for mass distributions of each nuclide according to the size of fly ash particles, general consideration on the mechanisms of particle formation can be used for predicting them in radwaste thermal process aerosol.

3.3. Correction Methods for Anisokinetic Sampling

It is considered here that a sample probe with nozzle cross section A_p situated in a stack or in a duct where the off-gas velocity is v_g and the particulate concentration is $C_{m,g}$. If a sample is withdrawn through a probe nozzle at a suction velocity v_s, which is not equal to v_g, a particulate mass m_p(kg) collected in a sampling time τ(s) gives a sample particulate mass flow rate $Q_{m,s}=m_p/\tau$. A sample concentration $C_{m,s}$ can be obtained as the ratio of the particulate mass flow rate in the probe Q_p(kgs^{-1}) divided by the volumetric flow rate through the probe v_sA_p:

$$C_{m,s}=\frac{Q_{m,s}}{v_s A_p} \tag{4}$$

Normally the suction velocity becomes smaller than originally set isokinetic sampling rate due to accumulation of sampled particle, which increases pressure drop across filter. If the suction velocity v_s is smaller than off-gas velocity v_g, or sampling is underisokinetic as shown in Fig. 2(b), the volumetric flow rate of gas is v_sA_p and the particulate mass flow rate is $v_sA_pC_{m,g}$. The flow rate that would have entered the probe if sampling were isokinetic but does not enter is $v_gA_p-v_sA_p$. The total mass flow rate of the particles in this gas stream of the probe is $(v_gA_p-v_sA_p)C_{m,o}$. If we assume that a fraction $\alpha(-)$ of these particles has sufficient inertia to diverge from gas streamlines and enter the probe, the particle mass flow rate in the probe is given by:

$$Q_{m,s}=v_sA_pC_{m,g}+\alpha C_{m,g}(v_gA_p-v_sA_p) \tag{5}$$

Eq. (5) is solved for $C_{m,o}$ with Q_p replaced by m_p/τ,

$$C_{m,g}=\frac{\frac{m_g}{\tau}}{\alpha v_gA_p+(1-\alpha)v_sA_p} \tag{6}$$

Thus the relation between the measured concentration $C_{m,s}$ to the true concentration $C_{m,g}$ is obtained from Eq. (4) and (6),

$$C_{m,s}=\alpha C_{m,g}\frac{v_g}{v_s}+(1-\alpha)C_{m,g} \tag{7}$$

A similar derivation gives identical equations for over-isokinetic sampling, $v_s>v_g$. For isokinetic sampling, Eq. (7) gives the expected result $C_{m,s}=C_{m,o}$. Badzioch [19] applied impaction theory to derive a theoretical expression for inertial parameter α in Eq. (7):

$$\alpha=\frac{1-\exp(-\frac{L_d}{\lambda})}{\frac{L_d}{\lambda}} \tag{8}$$

where L_d is the distance from the entrance to upstream of the probe at which the gas flow streamlines begin to diverge from their normal path. Experimentally determined λ and L_d are given by the following Eqs. (9) and (10) [19].

$$\lambda=\frac{(\rho_p-\rho_g)d_pv_s}{\mu} \tag{9}$$

$$L_d=C-1.6D_p \tag{10}$$

where L_d and D_p are both in centimeters. Eq. (10) has 95% confidence limits when the parameters are 5.2 to 6.8 for the constant C and 1.0 to 2.2 for the coefficient of D.

3.4. Sample Calculation

Density and viscosity of simulated vitrification melter off-gas with respect to temperature are shown in Table 1. Simulated gas composition and the properties of incinerator off-gas, which are also shown in Table 1, are used to calculate fractional deposition of particle in the sample transport tube in the following section. These transport properties were calculated by

using the predicting methods proposed by Richard [20]. The probe diameter and off-gas velocity were taken to be 0.025m and 10m/sec, respectively. Applied disturbance length L_d is 2cm by taking constant C to be 6. Inertial parameters for each nuclides and elements for vitrification melter aerosols [21] are calculated by particle mass fraction $w_i(-)$ and effective inertial parameter α_i for ith size group.

$$\alpha = \sum w_i \alpha_i \tag{11}$$

The values of α of each element in vitrification melter aerosol calculated in this manner are shown in Table 2. Average particle size of submicron particles were taken to be 0.5 microns. Two important findings from the calculation are that for most nonvolatile elements, α increases from about 0.3 to 0.6 as the temperature decreases 873 K to 373 K and for semivolatile nuclides (Cd, Cs and Te), inertial parameter $\alpha \simeq 0$ and hence from Eq. (8) $C_{m,s} \simeq C_{m,g}$ regardless of velocity ratio (v_o/v_s). With given values of for nonvolatile element or nuclides in Table 2, the true concentration in the process off-gas $C_{m,o}$ can be determined

Table 1. Simulated Off-gas Properties of Vitrification Melter and Incinerator

off-gas source	vitrification melter		incinerator	
simulated gas composition (vol %) [24]				
O_2	11		7	
N_2	32		70	
CO_2	50		12	
H_2O	8		11	
calculated properties ($\times 10^3$)				
at 1 atm	density ($g cm^{-3}$)	viscosity ($g cm^{-3} s^{-1}$)	density ($g cm^{-3}$)	viscosity ($g cm^{-3} s^{-1}$)
and 373 K	9.2	1.9	7.5	2.0
473 K	7.6	2.3	6.2	2.4
573 K	6.4	2.6	5.3	2.7
673 K	5.6	3.1	4.6	3.1
773 K	5.0	3.4	4.1	3.4

Table 2. Calculated Inertial Parameter for Vitrification Melter Aerosols

Element	Average Size Distributions(μm)				α in Given Off-gas Temperature (K)				
	16	6	1	<1	873	773	673	573	473
Al	96.2	0.9	2.5	0.4	0.48	0.51	0.56	0.59	0.64
B	87.8	1.8	7.8	2.6	0.44	0.46	0.51	0.54	0.58
Ba	83.7	5.8	10.5	0	0.42	0.45	0.49	0.52	0.56
Ca	77.7	2.7	15.2	4.4	0.39	0.41	0.45	0.48	0.52
Cd	10.7	0.8	7.3	81.2	0.05	0.06	0.06	0.07	0.07
Ce	92.1	0	7.9	0	0.46	0.49	0.53	0.56	0.61
Cs	7.5	0	5.4	87.1	0.04	0.04	0.04	0.05	0.05
Fe	77.3	2.6	17	3.1	0.39	0.41	0.45	0.48	0.52
La	91.9	1.5	6.1	0.5	0.46	0.49	0.53	0.56	0.61
Li	83.2	1.5	5.3	10	0.42	0.44	0.48	0.51	0.55
Mg	91.5	1.6	5.8	1.1	0.46	0.48	0.53	0.56	0.61
Mn	89.4	6.4	3.6	0.6	0.45	0.48	0.52	0.56	0.60
Na	68.8	1.7	5.6	23.9	0.35	0.36	0.40	0.42	0.46
Nd	93.4	0	6.6	0	0.47	0.49	0.54	0.57	0.62
Se	56.9	1.9	11.4	29.8	0.29	0.30	0.33	0.35	0.38
Si	92	1.8	5.6	23.9	0.46	0.49	0.53	0.57	0.61
Sr	77.6	2.8	19.6	0	0.39	0.41	0.45	0.48	0.52
Te	5.5	0.4	3.2	90.9	0.03	0.03	0.03	0.04	0.04
Ti	91.2	1.8	6	1	0.46	0.48	0.53	0.56	0.61
Zr	91.6	1.6	5.6	1.2	0.46	0.48	0.53	0.56	0.61

by anisokinetic sampling velocity ratio (v_o/v_s) and measured concentration $C_{m,s}$ by using Eq. (8).

3.5. Errors due to nonisoaxial sampling

Sampling errors can also be increased by nonisoaxial sampling. We can evaluated this effect by referring to several works by Fuchs [22, 23], Durham and Lundgren [24], and Tufto and Willeke [25]. Their common findings are as follows : the errors increase with Stokes number and angle between flow direction and nozzle direction of the probe ; thick shape of the probe also disturbs the flow field and will cause errors. It is more preferable to have a sharp edge at the probe entrance and keep the wall as thin as possible [26, 27].

4. Predictions of Particle Losses during Transport of Aerosols

Sampled radioactive aerosol must be transported to the site of the sample collection filter. It normally flows small round tubes. We normally ignore mass transfer such as volatilization and condensation between the gas and the particle phase, which can be normally occurring radwaste combustion aerosols. Even if we can ignore this small change in concentration by mass transfer between condensed to gas phase, the concentration of radioactive aerosol is still changing because of particle losses to the inside walls of sample transport tubes. The particle deposition can occur due to following five mechanisms [28] ;

- Browninan Diffusion
- Gravitational Settling
- Inertial Deposition
- Electrostatic Collection
- Thermophoretic Effects

Among five mechanisms, we can reduce electrostatic effect using well grounded metallic tubes and avoid thermophoretic effects by maintaining isothermal condition with external cooling or heating on the sampling lines. Depositions due to other three mechanisms, which we can not avoid more or less, depend on the flow characteristics, geometry and especially on particle size. These three effects are interdependent in some cases but are discussed here separatedly on two flow regime (laminar and turbulent). The extent of aerosol particle deposition in a sampling tube is defined here in terms of fractional deposition, $F_d(-)$:

$$F_d = 1 - \frac{(\frac{m_p}{V_g})_{out}}{(\frac{m_p}{V_g})_{in}} \tag{12}$$

where $m_p/V_g(kg/m^3)$ is particle mass in unit volume of sample gas and subscripts 'in' and 'out' denote the position of inlet and outlet of sample transport tube, respectively. Estimation methods for F_d are summarized here separatedly with sample flow characteristics.

4.1. Prediction of F_d in Laminar Flow

4.1.1. Gravitational Settling of Large Particle

Fractional deposition of relatively large particles by the gravity settling on a horizontal tube wall in a laminar flow regime is given by [29] :

$$F_d = 0.637\ [2\phi(1-\phi^{\frac{2}{3}})^{\frac{1}{2}} + \sin^{-1}\phi^{\frac{1}{3}}(1-\phi^{\frac{2}{3}})^{\frac{1}{2}}] \tag{13}$$

with dimensionless parameter $\phi = 0.375(L/r_p)(u_s/u)$, where $L(m)$ is the tube length, $r_p(m)$ the pipe radius, $u_s(m)$ settling velocity and $u(m)$ the mean gas velocity. Example plots for the gravitational depositions according to the particle size with simulated off-gas composition are shown in Fig. 4. Fractional depositions by gravitational settling increase with particle size but it decrease with temperature elevation.

4.1.2. Brownian Diffusion in Laminar Flow

Very small particles mainly deposit in a laminar

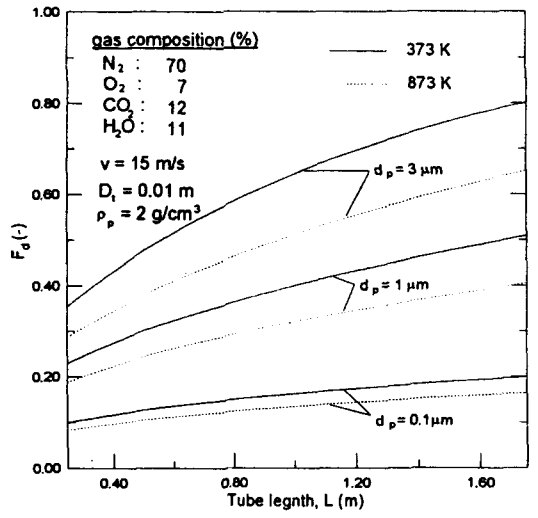

Fig 4. Gravitational Settling in a Sample Transport Tube

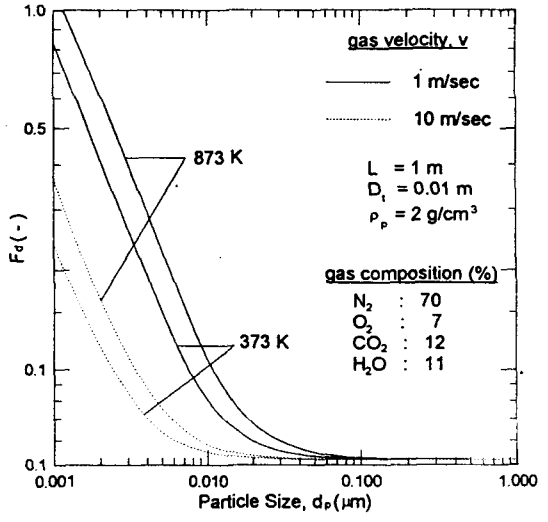

Fig 5. Brownian Deposition of Submicron Particle in a Sample Transport Tube

flow tube by the Brownian diffusion. In laminar flow regime following Eqs. (14) and (15) are generally accepted in given situations [30]:

for $\xi < 0.02$,

$$F_d = 1 - 0.819e^{-3.567\xi} + 0.097e^{-22.3\xi} + 0.032e^{-57\xi} \quad (14)$$

for $\xi > 0.02$,

$$F_d = -2.56\xi^{0.67} + 1.2\xi + 0.177\xi^{0.75} \quad (15)$$

where $\xi = \pi DL/Q_v$, $D(m^2s^{-1})$ diffusion coefficient and $Q_v(m^3s^{-1})$ the volumetric flowrate. Example plots for the fractional deposition against particle diameter and temperature in given gas velocity are shown in Fig. 5. In laminar flow, fractional deposition by Brownian diffusion increases with increase in temperature but it decreases with increase in gas velocity or increase in particle diameter.

4.2. Prediction of F_d in Turbulent Flow

In turbulent flow, Brownian diffusion is usually a significant removal process only for a ultrafine particles while inertial removal in turbulent flows is effective for relatively large particles larger than $1\mu m$. Brownian diffusion occurs when ultrafine particles diffuse across to laminar sublayer and stick to the wall. Inertial impaction occurs when particles have sufficient inertia to penetrate through the fluid boundary layer to the wall. Fractional deposition for turbulent regime could be obtained by [31]:

$$F_d = 1 - \exp\left(-\frac{v_+ u_* \pi D_t L_t}{Q_v}\right) \quad (16)$$

where v_+ dimensionless particle deposition velocity ($=v/u_*$), D_t(m) tube diameter, v(m/s) deposition velocity, u_* friction velocity ($=u\sqrt{f/2}$), u gas velocity, f (−) fanning friction factor ($=0.316/(4Re^{0.25})$), and L_t (m) tube length.

4.2.1. Brownian Diffusion in Turbulent Flow

Predictions of particle deposition due to Brownian diffusion under turbulent flow were made several authors. Davies [32] calculated deposition rate of particles diffusing by Brownian motion and by eddy diffusion. Equation for prediction of diffusion by Davis is somewhat complicated. Wells and Chamberlain [33], Friedlander [34] and Brockmann [35] used the

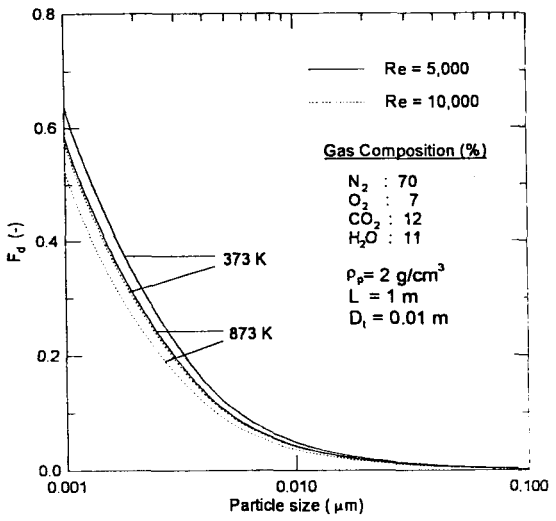

Fig 6. Deposition of Submicron Partcles Due to Brownian and Eddy Diffusion Under Turbulent Flow Conditions

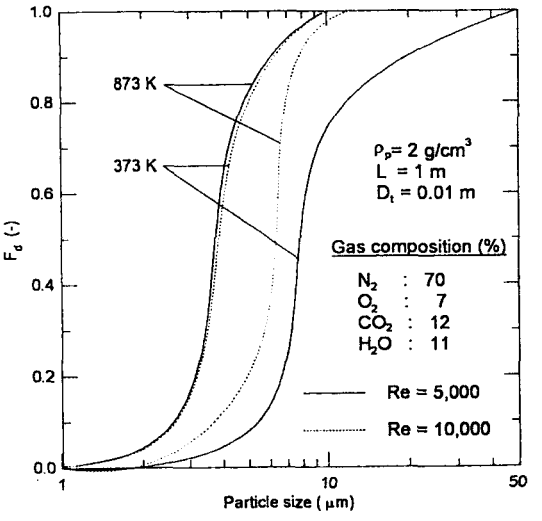

Fig 7. Deposition of Particle Due to Turbulent Iimpaction

following simple equation for particle deposition velocity by diffusion;

$$v_{+d}=0.2Sc^{-0.66}Re^{-0.125} \tag{17}$$

where v_{+d} dimensionless deposition velocity due to diffusion (v_d/u^*), v_d(m/s) deposition velocity due to diffusion, Sc Schmidt number($=\nu/D$), ν(m^2s^{-1}) Kinematic viscosity of the gas and D diffusion coefficient of the particle. Example plots for Brownian and eddy deposition in the turbulent flow is shown in Fig. 6. The fractional deposition due to Brownian and eddy diffusion, which is effective for small condensed particles such as Cd, Cs and Te, increases with decrease in particle diameter but changes relatively little due to changes in temperature or gas velocity.

4.2.2. Inertial Impaction

Friedlander and Johnston [36] and Liu and Agarwal [37] obtained a relation between a dimensionless deposition velocity by inertial impaction v_{+i} and relaxation time $\tau_+(-)$:

$$v_{+i}=0.0006\tau_+^2 \tag{18}$$

In Eq. (18) + has the following definition;

$$\tau_+=\frac{\tau_r u_f^2}{\nu} \tag{19}$$

with the relaxation time $\tau_r(=d_p^2\rho_P\rho_g/18\nu)$. Example plot for fractional deposition due to turbulent impaction are shown in Fig. 7. Particle losses due to inertial impaction in turbulent flow increase with increase in particle size or in temperature. For higher gas velocity and smaller particles, the temperature effect becomes smaller.

4.3. Deposition in Tube Bend

It is sometimes necessary to use tube bends in order to transport radioactive aerosol sample to radioactivity detection instrument. In this situation, we can also predict fractional deposition by Stokes number. Cheng and Wang experimentally observed fractional deposition in a 90° bend is equal to Stokes number [38];

$$F_d=Stk \tag{20}$$

for large curvature ratio R ($R=R_b/R_P>20$), where R_b and R_p are radii of the bend and the probe, respect-

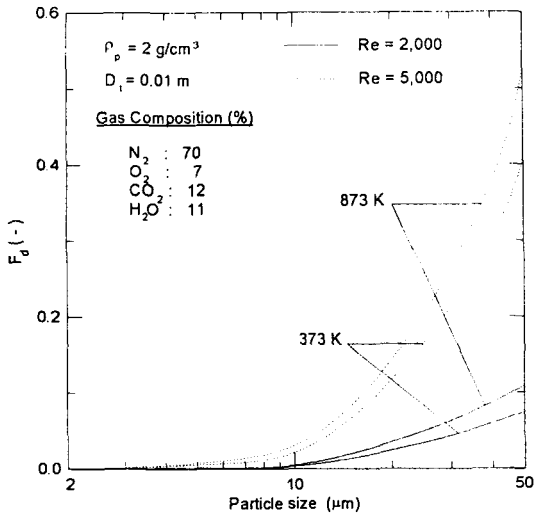

Fig 8. Losses of Particle in a 90° Bend Under Laminar and Turbulent Conditions

ively. Eq. (20) can be accepted only for small Stokes Number ($S_{tk}<0.1$) and high velocity ($Re>1000$). For very low Reynolds numbers, Pui [39] suggested that the Stokes number should be small in order to have negligible particle losses in bends. For turbulent flow, deposition in a bend occur both by turbulence and by centrifugal forces. He observed experimentally the fractional deposition in 90° bends under high transport velocity condition and the expressions is as follows.

$$F_d = 1 - 10^{0.963 St} \tag{21}$$

Eq. (21) are plotted in Fig. 8. Particle losses in bends increase with temperature and particle diameter. The higher gas velocity also results in more particle losses in bend. The Stokes number or transport velocity should be kept small for large particles in order to have negligiable particle depostion in bend.

5. Concluding Remarks

Mass distribution of entrained each radionuclide in aerosol particles largely depends upon its entrained mechanisms in the furnace or melter. As shown in Table 2, semivolatile nuclides, Cd, Cs and Te end up mostly as submicron particles while other nonvolatile nuclides end up as relatively larger particles. In this concern, we can roughly predict the size distributions of aerosol particles including investigated nuclides according to volatility characteristics. Aerosol particles containing nonvolatile nuclides are large enough to deviate from gas stream lines under anisokinetic condition and their depositions occur by gravitational setling or turbulent impaction according to sample transport velocity. Instead, particles containing semivolatile nuclides are fine particles. Errors due to anisokinetic sampling of those fine particles are relatively small but their depositions in the sample transport tube are relatively large in normal sample transport velocity. However, if we have the size distributions of aerosol particles and mass transport properties of off-gas such as density and viscosity, we can predict or correct errors of sampling and transport according to the methods discussed in this paper.

References

1. J.H. Kim, "Technology Development for Radwaste Volume Reduction and Solidification (I)", KAERI-NEMAC/RR-159/95, I-15-I-28 (1995)
2. S.H. Park, "Study on the Establishment of Technical Standard of Radioactive Waste (Interim Report), KINS/GR-105, 5-94 (1995)
3. Badzioch, S, Bri. *J. of Appl. Phys.*, **10**, 26 (1959)
4. W.C.L. Hemeon and G.F. Haines, *Air Repair*, **4**, 159 (1959)
5. C.N. Davis, *Staub-Reinhalt. Luft* **28**(6), 219-225 (1968).
6. F.R. Rehm, *J. Air Pollut. Control Assoc.*, **6**(5), 199-204 (1957)
7. J. Hermann, "Staub in Turbulenter Gasströmung-Staubverteilung und Messtechnische Probenahme", Ph. D. Dissertation, 82, TU Muenchen (1976)
8. Vitols, V., *J. Air Pollut. Control Assoc.* **16**, 79 (1966)

9. Ruping, G., *Staub*, **28**, 137 (1968)
10. Levich, V.G. Physicochemical Hydrodynamics, Prentice Hall, Englewood Cliff, New jersey (1962)
11. Wood, N.B., *J. of Aerosol Sci*, **12**, 275-290
12. Papavergos, P.G. and Hedley, A.B. *Chem. Eng. Res.* **62**, 275-295
13. Yang, *et al*, "Vaporization and Deposition of Cadmium and Lead with PVC combustion", 1996 International Conference on Incineration and Thermal Treatment Process, Savannah, USA, May 8, (1996).
14. R.G. Barton, Clark W.D. and Seeker W.R., *Comb. Sci. & Tech.* **4**, 327-342 (1990).
15. H. Paul, "Particulate Sampling of Wigwam Burners", Forest Research Lab., Oregon State University, Carvallis 115 (1968).
16. C.N. Davis, *Bri. J. of Appl. Phys.*, **1**, 921 (1968)
17. A.S. Moore, *Combustion*, **3**(4), 28-30 (1963).
18. P.A. Toynbee and W.J.S. Parkes, *Int. J. of Air and Water Pollution*, **6**(2), 113-120 (1962).
19. J. Badzioch, *J. of Institute of Fuel*, **33**, 106 (1960)
20. S.B. Richard, *I & EC Process Design and Development*, **8**(2), 243-245 (1969)
21. R.W. Goles and C.M. Anderson, "LFCM Emission and Off-gas System performance for Feed Component Cesium" Proc. SPECTRUM '86, ANS, 1068-1084 (1986)
22. N.A. Fuchs, "The Mechanics of Aerosols", Pergamon Press, Oxford, 182 (1964).
23. N.A. Fuchs, *Atmospheric Environment*, **9**(8), 697-707 (1975)
24. M.D. Durham and D.A. Lundgren, *J. of Aerosol Science* **11**(2) (1980)
25. P.A. Tufto and K. Willke, "Sampling Efficiencies of Particulate Sampling Inlets", Aerosols in Science, Medicine and Technology, 9th GAeF-Conference, 231-236, Duisburg (1981)
26. E. Fernandes and P. Suter, *Brennstoff-Wäerme-Kraft*, **26**(12), 502-506 (1974).
27. A.B. Whiteley and L.E. Reed, *J. of Institute of Fuel*, **32**(2), 316-319 (1959).
28. S.K. Friedlander, "Smoke, Dust and Haze", Jonn Willy and Sons (1976)
29. J.W. Thomas, *J. of Air Pollution Control Association*, **8**, 32-34 (1958)
30. P. Gormley and M. Kennedy, "Diffusion from a Stream Flowing Through a Cylindrical Tube", Proceedings of the Royal Irish Academy 52A, 163-169 (1949)
31. K.W. Lee and J.A. Gieseke, *J. of Aerosol Science*, **25**(4), 706 (1994)
32. C.N. Davis, "Aerosol Science", Academic Press, London, 393-446 (1966)
33. A.C. Wells and A.C. Chamberlain, *Bri. J. of Appl. Phys.*, **18**, (1973)
34. S.K. Friedlander and H.F. Johnstone, *Industrial Engineering Chemistry*, **49**, (1957)
35. J.E. Brockmann, "Coagulation and Deposition of Ultrafine Aerosols in Turbulent Pipe Flow, Ph. D. Thesis, University of Minesota, Mechanical Department, Minnapolis (1981)
36. S.K. Friedlander, *Industrial and Engineering Chemistry*, **49**, 1151-1156 (1957)
37. B.Y.H. Liu and J.K. Agarwal, *J. of Aerosol Science*, **5**(2), 145-155 (1974)
38. Y.S. Cheng and C.S. Wang, *Atmospheric Environment*, **15**(3), 301-306 (1981)
39. D.Y.H. Pui, F. Romay-Novas and B.Y.H. Liu, *Aerosol Science and Technology*, **7**(3), 301-315 (1994)